Porous ionic liquids based on biocompatible CD-MOFs

Cintia M. Correa,[†,‡] Jocasta Avila,[†] Tracy El Achkar,[¶] Pauline André,[¶] Shi-Minh Loo,[§,‡] Stéphane Baudron,[¶] François-Xavier Legrand,[§] Sophie Fourmentin,[‡] and Margarida Costa Gomes[*,†]

†*Laboratoire de Chimie de l'ENS Lyon, CNRS and Université de Lyon, 46 allée d'Italie, 69364 Lyon, France*

‡*Unité de Chimie Environnementale et Interactions sur le Vivant, UCEIV, UR 4492, Université du Littoral-Côte d'Opale, 145 avenue Maurice Schumann, 59140 Dunkerque, France*

¶*Laboratoire de Chimie de la Matière Complexe, UMR 7140, Institut Le Bel, 4 rue Blaise, 67081 Strasbourg, France*

§*Université Paris-Saclay, CNRS, Institut Galien Paris-Saclay, 91400 Orsay, France*

E-mail: margarida.costa-gomes@ens-lyon.fr

Supplementary Information

Preparation of CD-MOFs

CD-MOF-1 γ-CD (1.30 g, 1 mmol) and KOH (450 mg, 8 mmol) were dissolved in H_2O (20 mL). The aqueous solution was filtered and MeOH (50 mL) was allowed to vapor diffuse into the solution. After 4 days, colorless cubic crystals, suitable for X-ray crystallographic analysis, were isolated, filtered, washed with isopropanol, and dried at 50 °C overnight before being stored in a desiccator (1.5 g, 87%). TGA analysis shows a first weight loss of 18% corresponding to the loss of water and alcohol solvate molecules. Subsequent weight loss above 250 °C corresponds to decomposition of the material. Elemental analysis (CHN) was performed on a fully dried sample. Calcd. for $(KOH)_2C_{48}H_{80}O_{40}$: C, 40.90; H, 5.86. Found: C, 40.29; H, 6.18.

CD-MOF-2 γ-CD (1.30 g, 1 mmol) and RbOH (820 mg, 8 mmol) were dissolved in H_2O (20 mL). The aqueous solution was filtered and MeOH (50 mL) was allowed to vapor diffuse into the solution After 4 days, colorless cubic crystals, suitable for X-ray crystallographic analysis, were isolated, filtered, washed with isopropanol, and dried at 50 °C overnight before being stored in a desiccator (1.5 g, 86%).TGA analysis shows a first weight loss of 13% corresponding to the loss water and alcohol solvate molecules. Subsequent weight loss above 250 °C corresponds to decomposition of the material. Elemental analysis (CHN) was performed on a fully dried sample. Calcd. for $(RbOH)_2C_{48}H_{80}O_{40}$: C, 38.38; H, 5.50. Found: C, 38.10; H, 5.79.

Characterization of CD-MOFs

X-Ray Diffraction

Powder X-ray diffraction patterns were recorded at 293 K on a Bruker D8 diffractometer using monochromatic Cu-Kα radiation with a scanning range between 4 and 40°, with the compound placed on a rotating Si low background sample holder. The calculated diagrams were generated with the Mercury® software based on reported single-crystal data.

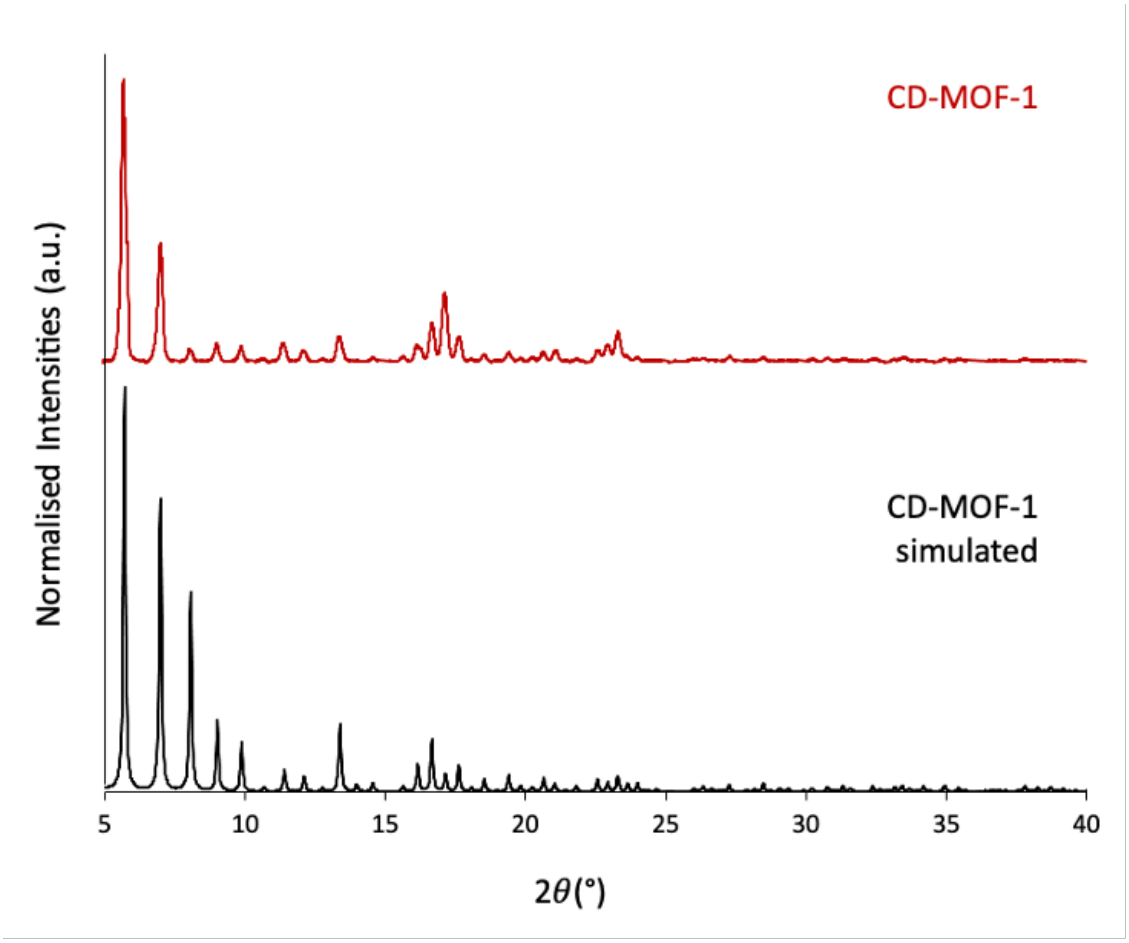

Figure S1: Powder X-Ray Diffraction of CD-MOF-1

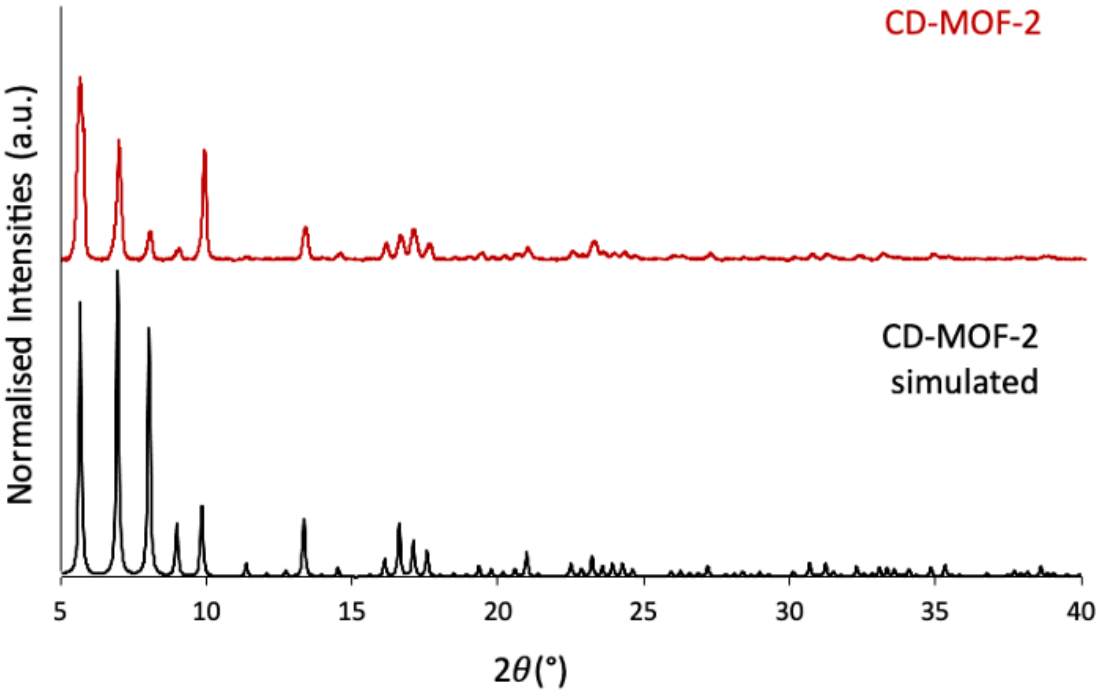

Figure S2: Powder X-Ray Diffraction of CD-MOF-2

Thermogravimetric analysis

The thermal stability of the samples was determined on a PerkinElmer thermogravimetric analyzer TGA 4000 under N_2 flow of 20 mL.min^{-1} and at a heating rate of 5 °C.min^{-1} up to 800 °C.

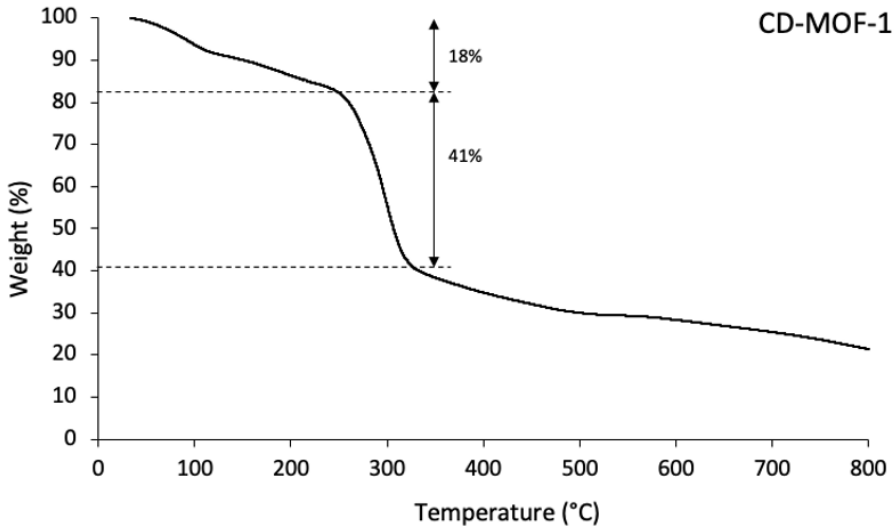

Figure S3: TGA of CD-MOF-1

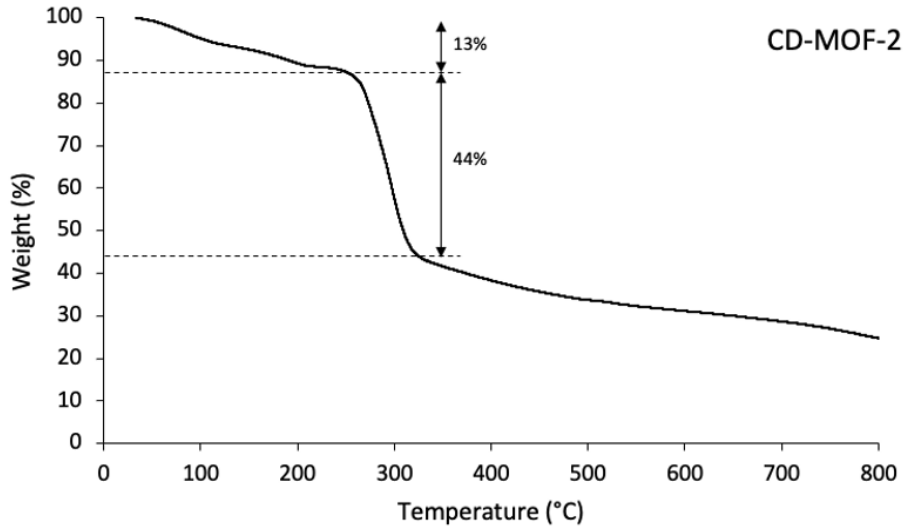

Figure S4: TGA of CD-MOF-2

Brunauer-Emmett-Teller (BET)

The textural properties of the samples were obtained by N_2 adsorption-desorption isotherms at 77 K, in a Micromeritics ASAP 2020 Surface Area and Porosity Analyzer. The Brunauer-Emmett-Teller (BET) method was used for obtaining the total specific surface area (SBET) and the pore size (model: NLDFT for cylinder pores). The samples were activated, prior to the N_2 adsorption-desorption analysis, first by three soaking in fresh CH_2Cl_2 for 24 h each, followed by heating the sample under vacuum at 50 °C for 12 h. The MicroActive Software version 4.00 was used to analyze the data.

Table S1: Brunauer-Emmett-Teller (BET).

MOF	CD-MOF-1	CD-MOF-2
BET Surface Area (m^2/g)	1024 ± 13	775 ± 10
C value	507	535
Correlation Coefficient	0.9996	0.9996
Total Pore Volume (cm^3/g)	0.3805	0.2874

Elemental Analysis

Elemental analyses (CHN) were performed at the Service Commun d'Analyses of the University of Strasbourg, in duplicate, employing a ThermoFischer Flash 2000 equipment.

Table S2: Elemental Analysis of CD-MOF-1.

Sample	%N	%C	%H
CD-MOF-1	0.00	40.0	6.15
	0.00	40.6	6.22
Theoretical values	0.00	40.9	5.86

Table S3: Elemental Analysis of CD-MOF-2.

Sample	%N	%C	%H
CD-MOF-2	0.00	38.3	5.78
	0.00	37.9	5.81
Theoretical values	0.00	38.4	5.50

Preparation of porous ionic liquids

The ionic liquids $[P_{6,6,6,14}][NTf_2]$, trihexyltetradecylphosphonium bis(trifluoromethylsulfonyl)-imide was supplied by Iolitec with purity >98 %. Preparation and characterization of the porous materials, CD-MOF-1 and CD-MOF-2, are detailed above.

Carbon dioxide, CO_2 was purchased from Messer with a mole fraction purity of 99.995 % from Air Liquide. The gas was used as received.

The PoILs, i.e. suspensions of CD-MOF-1 and CD-MOF-2 in $[P_{6,6,6,14}][NTf_2]$ were prepared at room temperature by weighing the components using a Mettler Toledo New Classic MS balance with an accuracy of ±0.01 mg, and by stirring the mixture at 500–600 rpm during 5 minutes at room temperature. Humidity can influence the structure of CD-MOFs, all samples were prepared and kept in an inert atmosphere in a glovebox containing argon.

Table S4: Sample nomenclature and composition used in the gas absorption measurements.

Sample	m_{liquid} (g)	$m_{\text{CD-MOF}}$ (g)	MOF %w/w
$[P_{6,6,6,14}][NTf_2]$			
$[P_{6,6,6,14}][NTf_2]$+CD-MOF-1	2.9021	0.14415	4.8706
$[P_{6,6,6,14}][NTf_2]$+CD-MOF-2	2.8398	0.14212	4.9779

Density measurements

The densities of the samples were measured in an Anton Paar DMA 5000M densimeter, in the temperature range 293–353 K at atmospheric pressure. The densimeter's working measurement is described in our previous works.[1] The maximum temperature deviation in the density measurements was ±0.01°C.

The knowledge of the densities of the liquid phases are essential to calculate the gas absorption values.

Table S5: Experimental densities of the PoILs $[P_{6,6,6,14}][NTf_2]$ + CD-MOF-1 or CD-MOF-2 5 % w/w, in the temperature range 293–353 K. The deviations indicated are relative to the fitting polynomials with coefficients listed in Table S6

T/K	ρ/g cm^{-3}	δ/%	T/K	ρ/g cm^{-3}	δ/%
$[P_{6,6,6,14}][NTf_2]$+ CD-MOF-1			$[P_{6,6,6,14}][NTf_2]$ + CD-MOF-2		
293.15	1.0769	−0.02	293.15	1.0869	−0.01
298.15	1.0734	−0.01	298.15	1.0833	−0.01
303.15	1.0699	+0.00	303.15	1.0797	+0.00
313.15	1.0628	+0.01	313.15	1.0726	+0.01
323.15	1.0559	+0.02	323.15	1.0655	+0.02
333.15	1.0490	+0.02	333.15	1.0584	+0.02
343.15	1.0423	+0.00	343.15	1.0515	+0.01
353.15	1.0358	−0.03	353.15	1.0449	−0.03

Table S6: Parameters A_0 and A_1 from linear functions used to fit the experimental densities, $\rho = A_0 + A_1 T$, as a function of temperature and absolute average deviation (AAD)

Sample	A_0/g cm^{-3}	A_1/g cm^{-3} K^{-1}	AAD/%
$[P_{6,6,6,14}][NTf_2]$+ CD-MOF-1	1.27825	$-6.874\,64 \times 10^{-4}$	0.02
$[P_{6,6,6,14}][NTf_2]$+ CD-MOF-2	1.29266	$-7.024\,86 \times 10^{-4}$	0.01

$AAD = \frac{100}{N} \sum_{i=1}^{N} \left(\frac{|\rho_{exp_i} - \rho_{cal_i}|}{\rho_{cal_i}} \right)$

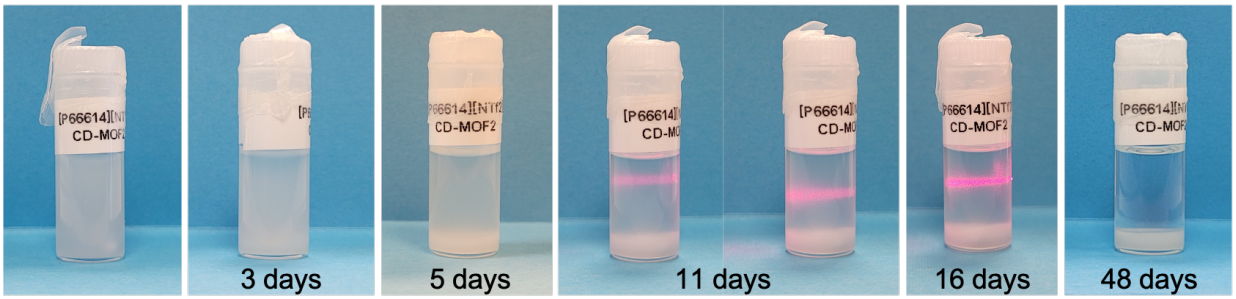

Figure S5: Visual appearance of PoIL prepared with CD-MOF-2 within 48 days and *Tyndall* Effect.

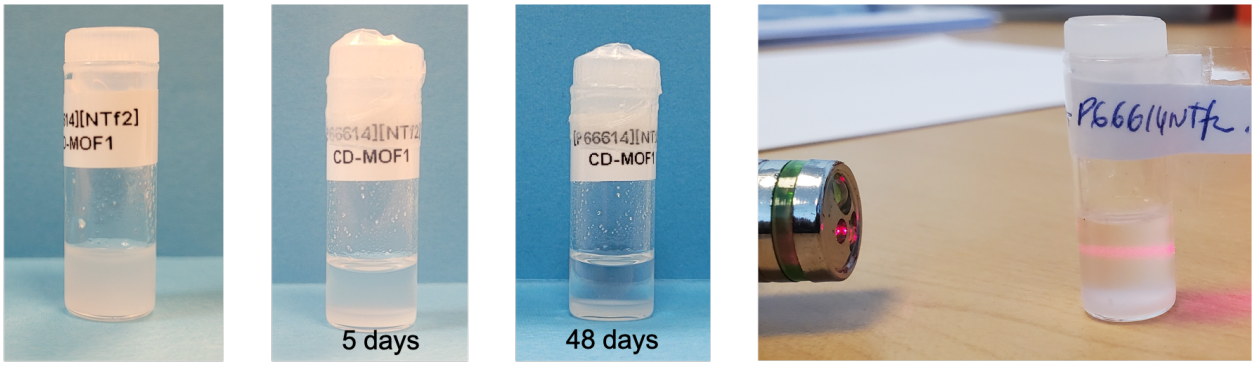

Figure S6: Visual appearance of PoIL prepared with CD-MOF-1 within 48 days and *Tyndall* Effect.

Gas absorption data

The gas absorption measurements were performed gravimetrically using an Intelligent Gravimetric Analyzer (IGA001) microbalance. The working principle and the data treatment are well described in our previous works.[1,2]

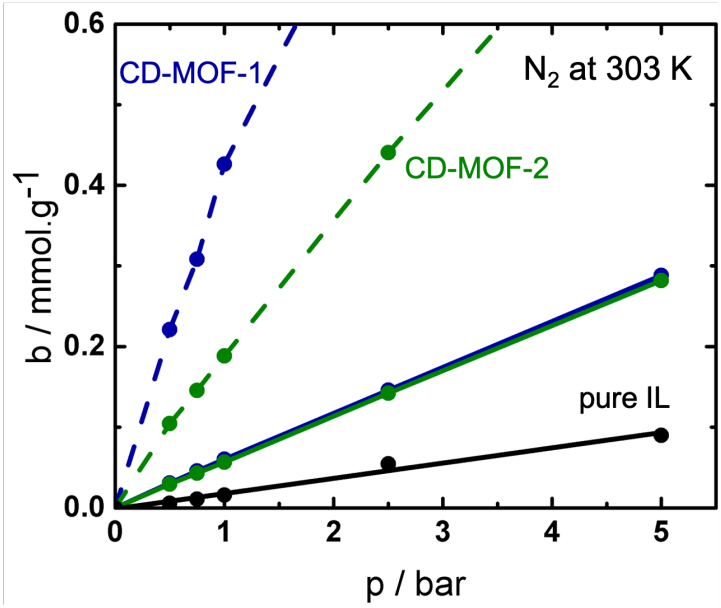

Figure S7: Absorption of N_2 in pure $[P_{6,6,6,14}][NTf_2]$, in the solid CD-MOFs and in the suspensions at 303 K and up to 5 bar. Differences in the absorption of solids (CD-MOF-1 and CD-MOF-2) may be related to exposure to atmospheric humidity. However, these differences are not observed when the solids are mixed with the ionic liquid, forming the PoILs. It might be due to the hydrophobicity of the liquid that keeps the CD-MOFs protected from humidity.

Table S7: Raw data (weight, pressure, and temperature) of absorption and desorption of CO_2 and N_2 by the pure IL, the porous liquid IL+CD-MOFs, and the porous solids as a function of pressure from 0.5–5 bar at 303.15 K.

T/K	p/bar	w/mg	T/K	p/bar	w/mg	T/K	p/bar	w/mg
			N_2 — Absorption					
$[P_{6,6,6,14}][NTf_2]$			$[P_{6,6,6,14}][NTf_2]$+CD-MOF-1			CD-MOF-1		
302.86	0.0000	101.7154	303.13	0.0000	45.64417	301.16	0.0000	16.51253
303.14	0.4994	101.6683	303.14	0.4984	45.63413	303.09	0.4989	16.59330
303.15	0.7481	101.6503	303.17	0.7487	45.62917	303.13	0.7487	16.62369
303.15	0.9983	101.6313	303.17	0.9991	45.62401	303.13	0.9992	16.66830
303.14	2.4876	101.5166	303.15	2.4999	45.58899	303.15	2.5002	16.79178
303.16	4.9855	101.3244	303.15	4.9991	45.52998	303.09	4.9987	16.92239
			N_2 — Desorption					
303.16	4.9855	101.3244	303.15	4.9991	45.52998	303.09	0.4998	16.92239
303.15	2.4985	101.5823	303.15	2.4999	45.59145	303.14	0.2498	16.76348
303.14	0.9976	101.6355	303.13	0.9975	45.62661	303.14	0.9993	16.64396
303.13	0.7479	101.6532	303.17	0.7481	45.63044	303.15	0.7487	16.61706
303.14	0.4989	101.6715	303.17	0.4978	45.63480	303.16	0.4982	16.58297
302.86	0.0000	101.7154	303.09	0.0000	45.64627	303.16	0.0000	16.38809
			N_2 — Absorption					
$[P_{6,6,6,14}][NTf_2]$			$[P_{6,6,6,14}][NTf_2]$+CD-MOF-2			CD-MOF-2		
303.15	0.0000	101.7154	303.16	0.0000	46.56039	302.82	0.0000	17.73426
303.15	0.4992	101.6683	303.13	0.4986	46.54882	303.16	0.4971	17.76495
303.16	0.7480	101.6503	303.15	0.7489	46.54233	303.15	0.7484	17.77525
303.13	0.9979	101.6313	303.15	0.9996	46.53563	303.15	0.9993	17.78648
303.14	2.4930	101.5166	303.13	2.4997	46.50187	303.14	2.4991	17.85199
303.15	4.9855	101.3244	303.12	4.9993	46.44120	303.12	4.9998	17.94341
			N_2 — Desorption					
303.00	4.9855	101.3244	303.12	4.9993	46.44120	303.12	4.9998	17.94341
303.23	2.4985	101.5823	303.16	2.4997	46.50245	303.17	2.4994	17.85682
303.15	0.9976	101.6355	303.15	0.9993	46.53816	303.15	0.9989	17.79649
303.15	0.7479	101.6532	303.14	0.7492	46.54286	303.14	0.7478	17.78370
303.14	0.4989	101.6715	303.14	0.4964	46.54813	303.15	0.4972	17.76991
303.15	0.0000	101.7154	303.13	0.0000	46.55737	303.22	0.0000	17.67799
			CO_2 — Absorption					
$[P_{6,6,6,14}][NTf_2]$			$[P_{6,6,6,14}][NTf_2]$+CD-MOF-1			CD-MOF-1		
303.00	0.0000	128.88670	303.25	0.0000	45.62257	301.48	0.0000	16.41806
303.23	0.4988	128.95140	303.10	0.4974	45.68840	303.13	0.4992	17.74340
303.15	0.7492	128.98090	303.14	0.7487	45.70604	303.14	0.7488	17.90193
303.15	0.9986	129.00890	303.17	0.9995	45.72464	303.15	0.9995	18.04168

$\frac{T}{\mathrm{K}}$	$\frac{p}{\mathrm{bar}}$	$\frac{w}{\mathrm{mg}}$	$\frac{T}{\mathrm{K}}$	$\frac{p}{\mathrm{bar}}$	$\frac{w}{\mathrm{mg}}$	$\frac{T}{\mathrm{K}}$	$\frac{p}{\mathrm{bar}}$	$\frac{w}{\mathrm{mg}}$
303.14	2.4977	129.18070	303.14	2.4996	45.82797	303.15	2.4992	18.64202
303.15	4.9967	129.46350	303.16	4.9989	46.00154	303.14	4.9982	19.30632
				CO_2 — Desorption				
303.00	4.9969	129.46350	303.25	4.9989	46.00154	301.48	4.9982	19.30632
303.23	2.4986	129.18230	303.10	2.4989	45.83327	303.13	2.4996	18.64976
303.15	0.9978	129.00920	303.14	0.9989	45.72985	303.14	0.9996	18.04326
303.15	0.7485	128.98290	303.17	0.7492	45.71085	303.15	0.7486	17.90874
303.14	0.4992	128.95370	303.14	0.4978	45.69051	303.15	0.4977	17.75323
303.15	0.0000	128.89460	303.16	0.0000	45.63700	303.14	0.0000	16.43721
				CO_2 — Absorption				
$[P_{6,6,6,14}][NTf_2]$			$[P_{6,6,6,14}][NTf_2]$+CD-MOF-2			CD-MOF-2		
303.00	0.0000	128.8867	304.59	0.0000	46.56500	303.15	0.0000	17.68342
303.23	0.4988	128.9514	303.15	0.4979	46.61488	303.00	0.4988	18.95492
303.15	0.7492	128.9809	303.23	0.7485	46.63582	303.00	0.7473	19.09983
303.15	0.9986	129.0089	303.08	0.9996	46.65155	303.00	0.9993	19.22803
303.14	2.4977	129.1807	303.15	2.5002	46.75248	303.00	2.4991	19.77927
303.15	4.9967	129.4635	303.14	4.9977	46.92136	303.00	4.9995	20.40701
				CO_2 — Desorption				
303.00	4.9969	129.46350	303.25	4.9977	46.92136	301.48	4.9995	20.40701
303.23	2.4986	129.18230	303.10	2.4988	46.75712	303.13	2.4981	19.78957
303.15	0.9979	129.00920	303.14	0.9988	46.65526	303.14	0.9984	19.23787
303.15	0.7485	128.98290	303.17	0.7489	46.63624	303.15	0.7480	19.10711
303.14	0.4992	128.95370	303.14	0.4985	46.61640	303.15	0.4982	18.96093
303.15	0.0000	128.89460	303.16	0.0000	46.56177	303.14	0.0000	17.76147

Table S8: Absorption and desorption (b in mmol/g) of CO_2 and N_2 by the pure IL, the porous liquid IL+CD-MOFs, and the porous solids as a function of pressure from 0.5–5 bar at 303.15 K.

T/K	p/bar	b/mmol g^{-1}	T/K	p/bar	b/mmol g^{-1}	T/K	p/bar	b/mmol g^{-1}
				N_2 — Absorption				
$[P_{6,6,6,14}][NTf_2]$			$[P_{6,6,6,14}][NTf_2]$+CD-MOF-1			CD-MOF-1		
302.86	0.0000	0.00000	303.13	0.0000	0.00000	303.16	0.0000	0.00000
303.14	0.4994	0.00519	303.14	0.4984	0.03081	303.09	0.4989	0.22096
303.15	0.7481	0.01024	303.17	0.7487	0.04574	303.13	0.7487	0.30822
303.15	0.9983	0.01501	303.17	0.9991	0.06053	303.13	0.9992	0.42627
303.14	2.4877	0.04286	303.15	2.4999	0.14606	303.15	2.5002	0.82279
303.16	4.9855	0.08968	303.15	4.9991	0.28820	303.09	4.9987	1.32106
				N_2 — Desorption				
303.16	4.9855	0.08968	303.15	4.9991	0.28820	303.09	4.9987	1.32106
303.15	2.4984	0.06641	303.15	2.4999	0.14798	303.14	2.4989	0.76151
303.14	0.9976	0.01646	303.13	0.9975	0.06245	303.14	0.9993	0.37366
303.13	0.7479	0.01126	303.17	0.74815	0.04669	303.15	0.7487	0.29388
303.14	0.4989	0.00630	303.17	0.4978	0.03128	303.16	0.4982	0.19857
302.86	0.0000	0.00000	303.08	0.0000	0.00000	303.16	0.0000	0.00000
				N_2 — Absorption				
$[P_{6,6,6,14}][NTf_2]$			$[P_{6,6,6,14}][NTf_2]$+CD-MOF-2			CD-MOF-2		
303.15	0.0000	0.0000	303.16	0.0000	0.00000	302.82	0.0000	0.00000
303.15	0.4992	0.0057	303.13	0.4986	0.02935	303.16	0.4971	0.10469
303.16	0.7480	0.0107	303.15	0.7489	0.04298	303.15	0.7484	0.14556
303.13	0.9979	0.0157	303.15	0.9996	0.05647	303.15	0.9993	0.18828
303.14	2.4930	0.0547	303.13	2.4997	0.14216	303.14	2.4991	0.44040
303.15	4.9855	0.0899	303.12	4.9993	0.28181	303.12	4.9998	0.82512
				N_2 — Desorption				
303.15	0.0000	0.0000	303.12	4.9992	0.28181	303.12	4.9998	0.82512
303.15	0.4992	0.0057	303.16	2.4998	0.14259	303.17	2.4994	0.45014
303.16	0.7480	0.0107	303.15	0.9993	0.05839	303.15	0.9989	0.20840
303.13	0.9979	0.0157	303.14	0.7495	0.04340	303.14	0.7479	0.16253
303.14	2.4930	0.0547	303.14	0.4964	0.02865	303.15	0.4972	0.11468
303.15	4.9855	0.0899	303.13	0.0000	0.00000	303.22	0.0000	0.00000
				CO_2 — Absorption				
$[P_{6,6,6,14}][NTf_2]$			$[P_{6,6,6,14}][NTf_2]$+CD-MOF-1			CD-MOF-1		
303.00	0.0000	0.00000	303.25	0.0000	0.00000	301.48	0.0000	0.00000
303.23	0.4988	0.03389	303.10	0.4974	0.06507	303.13	0.4992	1.89247
303.15	0.7492	0.04997	303.14	0.7487	0.08772	303.14	0.7488	2.13421
303.15	0.9986	0.06577	303.17	0.9995	0.11084	303.15	0.9995	2.35006

$\frac{T}{\mathrm{K}}$	$\frac{p}{\mathrm{bar}}$	$\frac{b}{\mathrm{mmol\,g^{-1}}}$	$\frac{T}{\mathrm{K}}$	$\frac{p}{\mathrm{bar}}$	$\frac{b}{\mathrm{mmol\,g^{-1}}}$	$\frac{T}{\mathrm{K}}$	$\frac{p}{\mathrm{bar}}$	$\frac{b}{\mathrm{mmol\,g^{-1}}}$
303.14	2.4977	0.16185	303.14	2.4996	0.24567	303.15	2.4992	3.31575
303.15	4.9967	0.32320	303.16	4.9989	0.4728	303.14	4.9982	4.46173
				CO_2 — Desorption				
303.15	4.9969	0.32320	303.22	4.9989	0.47281	301.48	4.9982	4.46173
303.15	2.4986	0.16217	303.12	2.4989	0.24827	303.13	2.4996	3.32651
303.16	0.9979	0.06580	303.14	0.9989	0.11340	303.14	0.9996	2.35226
303.13	0.7485	0.05030	303.14	0.7493	0.09015	303.15	0.7486	2.14360
303.14	0.4992	0.03431	303.13	0.4978	0.06614	303.15	0.4977	1.90593
303.15	0.0000	0.00000	303.16	0.0000	0.00000	303.14	0.0000	0.00000
				CO_2 — Absorption				
$[P_{6,6,6,14}][NTf_2]$			$[P_{6,6,6,14}][NTf_2]$+CD-MOF-2			CD-MOF-2		
303.00	0.0000	0.00000	304.59	0.0000	0.00000	303.15	0.0000	0.00000
303.23	0.4988	0.03389	303.15	0.4979	0.05620	303.00	0.4988	1.68779
303.15	0.7492	0.04997	303.23	0.7485	0.08007	303.00	0.7473	1.89461
303.15	0.9986	0.06577	303.08	0.9996	0.10145	303.00	0.9993	2.08027
303.14	2.4977	0.16185	303.15	2.5002	0.23302	303.00	2.4991	2.91362
303.15	4.9967	0.32320	303.14	4.9977	0.45426	303.00	4.9995	3.93052
				CO_2 — Desorption				
303.15	4.9969	0.32320	303.22	4.9977	0.45426	301.48	4.9995	3.93052
303.15	2.4986	0.16217	303.12	2.4988	0.23521	303.13	2.4981	2.92678
303.16	0.9979	0.06580	303.14	0.9988	0.10321	303.14	0.9984	2.09284
303.13	0.7485	0.05030	303.14	0.7489	0.08030	303.15	0.7480	1.90402
303.14	0.4992	0.03431	303.13	0.4985	0.05698	303.15	0.4982	1.69546
303.15	0.0000	0.00000	303.16	0.0000	0.00000	303.14	0.0000	0.00000

X Ray Diffraction Analysis - XRD

The XRD patterns were measured using a Malvern Panalytical Empyrean X-ray diffractometer (Cu Kα radiation at 0.154184 nm) equipped with a Ni filter and a PIXcel3D detector. The data were collected over a range of 5° to 40° (2θ), with a scan speed of 0.5° min^{-1} and a step width of 0.02°.

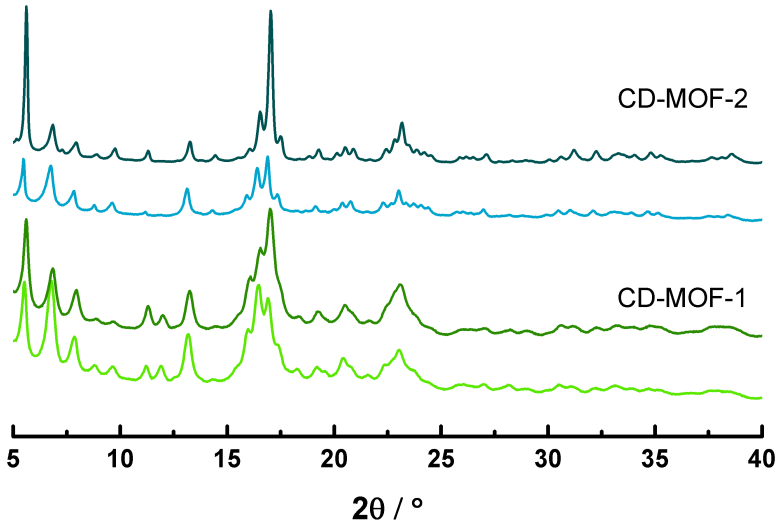

Figure S8: XRD of CD-MOF-1 and CD-MOF-2 before (dark green and dark blue for CD-MOF-1 and CD-MOF-2, respectively) and after grinding (light green and light blue for CD-MOF-1 and CD-MOF-2, respectively) under Argon atmosphere.

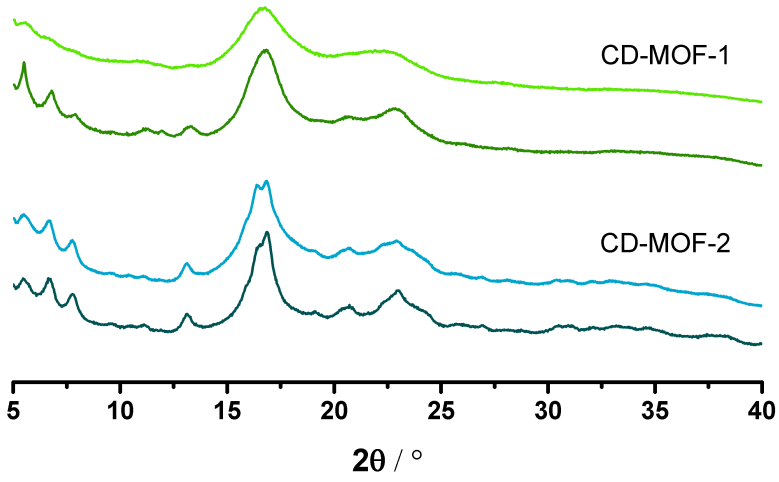

Figure S9: XRD of CD-MOF-1 and CD-MOF-2 before (dark green and dark blue for CD-MOF-1 and CD-MOF-2, respectively) and after grinding (light green and light blue for CD-MOF-1 and CD-MOF-2, respectively) under atmospheric conditions.

Small-angle X-ray scattering

Small-angle X-ray scattering (SAXS) measurements were carried out on an X-ray scattering instrument XENOCS Xeuss 3.0. The experiments were performed at a wavelength of 1.542 Å. Glass capillaries of 1 mm containing pure ionic liquids and their respective suspensions with 5 % w/w ZIF-8 were prepared and sealed with the aid of a flame, all of which were subsequently checked using a primary vacuum line. The capillaries were placed in the sample holder and the chamber was evacuated to 0.1 mbar vaccum to allow the detector to get closer to the samples and to limit parasitic diffusion maintaining a good signal to noise ratio. The sample to SAXS detector distance was 94.8 mm, recording a q range of 0.01–2.5 $Å^{-1}$, and the measurements acquired during 3600 s. After the acquisition, beamline-specific corrections were applied to the SAXS images and the intensity was radially averaged to yield intensity as a function of the wavevector. An empty capillary was also recorded in the same conditions and subtracted from all the samples. Data treatment was performed using XSACT 2.10.3 software.

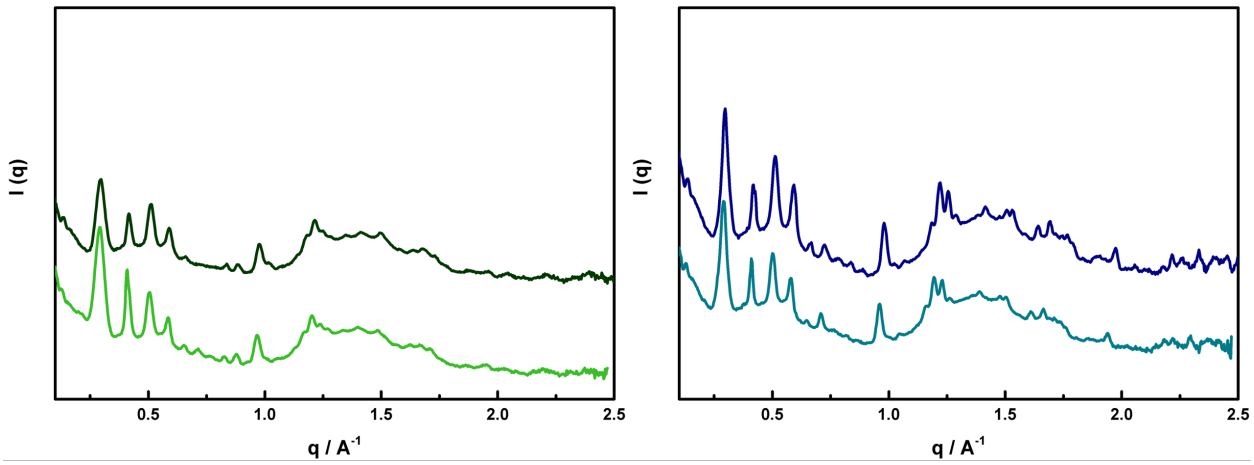

Figure S10: SAXS structure factor of CD-MOF-1 and CD-MOF-2 in $[P_{6,6,6,14}][NTf_2]$ freshly prepared (light green and light blue for CD-MOF-1 and CD-MOF-2, respectively) and 60 days after the preparation (dark green and dark blue for CD-MOF-1 and CD-MOF-2, respectively).

Turbiscan measurements

The sedimentation of the suspensions was examined using a Turbiscan Classic MA 2000 apparatus. Approximately 6.0 mL of suspensions were prepared by mixing CD-MOF-1 or CD-MOF-2 and $[P_{6,6,6,14}][NTf_2]$. The samples were prepared inside an Argon glovebox. Then, they were removed from the inert atmosphere and transferred to the cylindrical tubes designed for this Turbiscan model. Measurements were taken at intervals of 10, 20, and 30 minutes, as well as after some hours and several days following preparation. All measurements were conducted at room temperature.

Figure S11 displays the transmittance over time, using CD-MOF-1 as an example, at different heights within the Turbiscan tube — specifically, near the bottom (7 mm), in the middle (25 mm), and at the top (43 mm). This plot allows us to observe how transmittance varies at these heights over time. Near the bottom of the tube, the initial transmittance is around 18 %, remaining relatively constant during the first three hours. However, after 20 hours, there is a slight increase, with transmittance rising from 18 % to 22 %. This value continues to rise gradually, reaching 46 % in the last measurement taken ten days after sample preparation. In contrast, the transmittance at the top of the bottle also starts at approximately 19 %, similar to the bottom. Yet, after three hours, a significant increase occurs, with transmittance rising from 19 % to 28 %. After 20 h getting around 60 % and after 3 days already up to 90 %. When measurements are taken from the middle of the tube, the variation in transmittance is only slightly different compared to the bottom of the tube. After ten days, the transmittance reaches a value of 53 %, which is significantly lower than the 98 % observed at the top of the tube. This indicates that even after ten days at an average height along the tube, a substantial amount of particles remains present. Overall, these measurements illustrate the differences in transmittance changes over time at various heights within the cylindrical glass tube. Transmittance also enables us to measure the sediment thickness at the bottom of the tube.

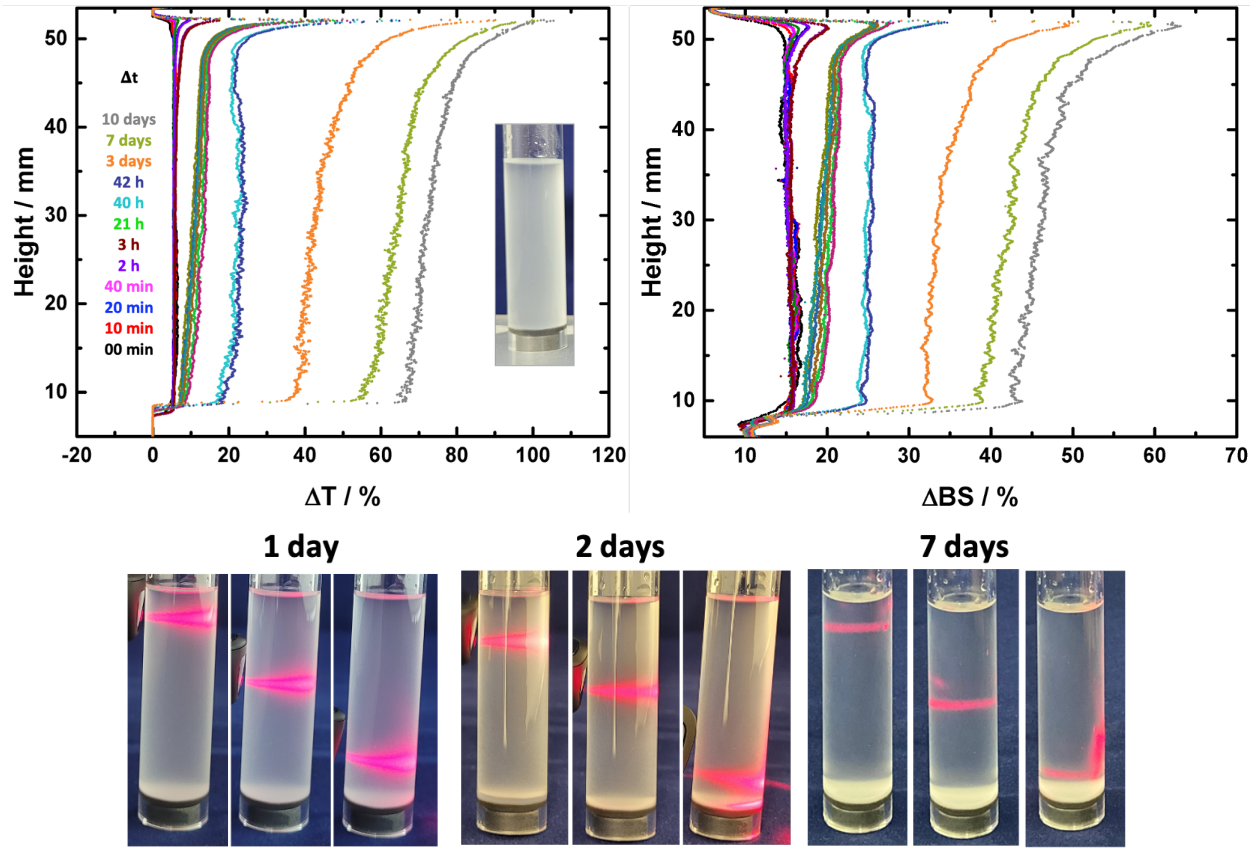

Figure S11: Turbiscan measurements of a suspension containing ≈ 1.0 % w/w of CD-MOF-2 in $[P_{6,6,6,14}][NTf_2]$ transmittance and back scattering over time.

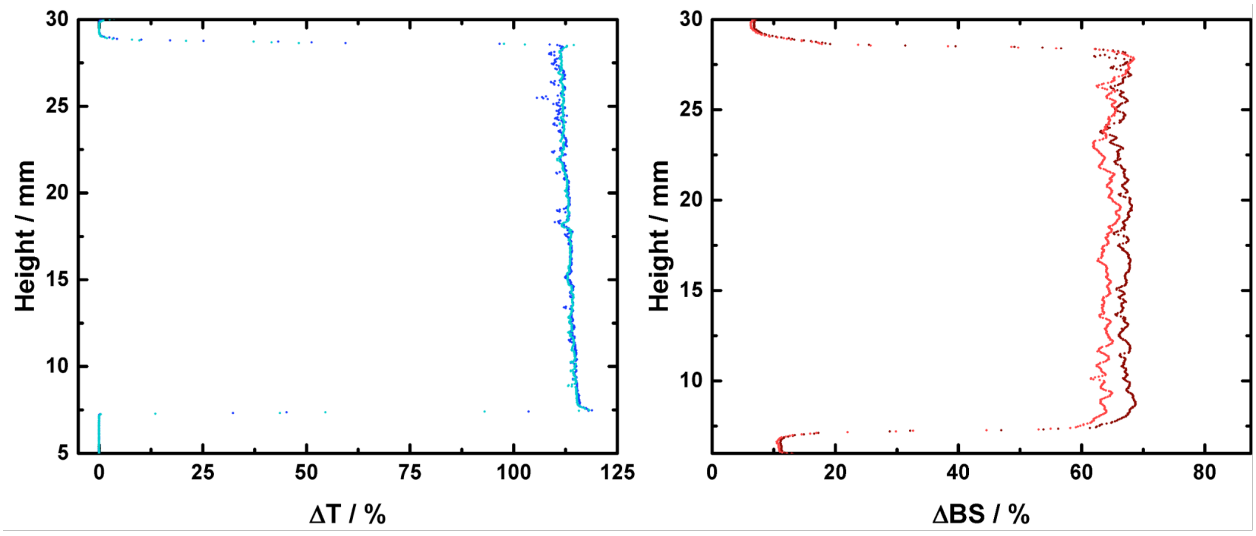

Figure S12: Turbiscan measurements of a pure ionic liquid $[P_{6,6,6,14}][NTf_2]$ transmittance and back scattering for time zero and after 2 hours.

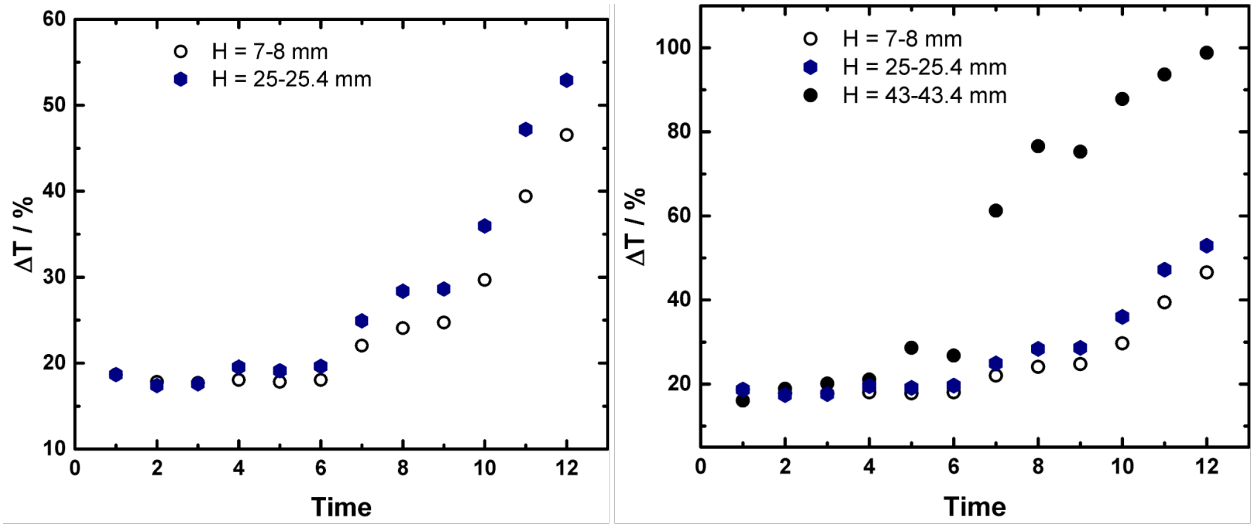

Figure S13: Transmittance over time at three different heights for CD-MOF-1 in $[P_{6,6,6,14}][NTf_2]$: 7-8 mm at the bottom, 25-25.4 in the middle and 43-43.4 at the top of the Turbiscan vial. The times represented by increasing numbers (1, 2, 3...) represent the times: zero minutes, 10 minutes, 20 minutes, 40 minutes, 2 hour, 3 hours, 20 hours, 40 hours, 42 hours, 3 days, 7 days and 10 days. (Left): only H = 7-8 mm and 25-25.4 mm and (right): all heights, in order to facilitate the visualization.

Dynamic Light Scattering

DLS measurements were perfomed in a Malvern Zetasizer Nano ZS at 298 K. The data were collected at the angle of 173° in the backscatter mode and were processed using the general purpose normal resolution option and using extend duration for large particles with relaxation time multiplier of 10^5. The samples were prepared in Argon inert atmosphere by adding 1.92 mg or 1.94 mg of CD-MOF-1 or CD-MOF-2 in 1.028918 g or 1.05341 g of $[P_{6,6,6,14}][NTf_2]$, respectively, resulting in a concentration of approximately 2 mg/mL.

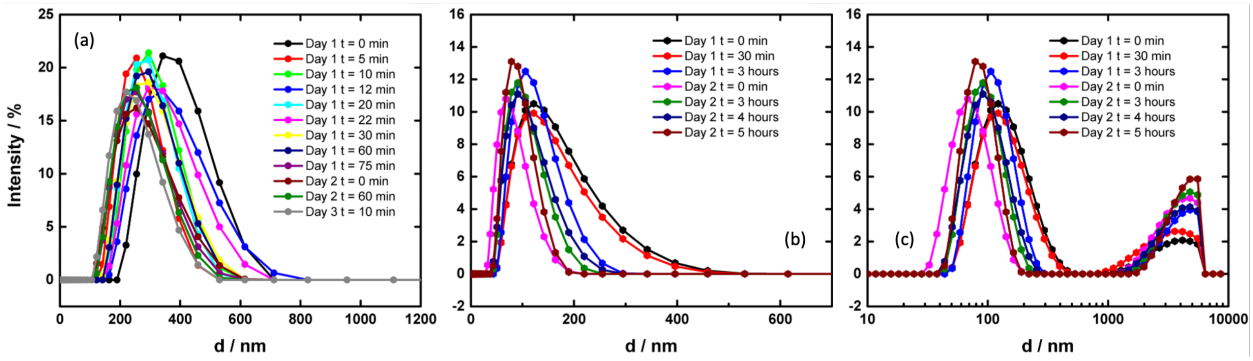

Figure S14: Dynamic light scattering of (a) CD-MOF-2 and (b-c) CD-MOF-1 PoILs in $[P_{6,6,6,14}][NTf_2]$ at 2 mg mL^{-1} concentration and 298 K.

Nuclear magnetic resonance

The Nuclear Magnetic Resonance (NMR) spectra of ^{1}H and ^{13}C were measured on a 400 MHz Bruker Avance III spectrometer. The equipment has a broadband Prodigy probe 5mm 1H-X gradient Z at 298 K.

In the NMR spectra shown below, we can observe the upper phase containing the ionic liquid after complete phase separation of the suspension prepared with CD-MOF-2 (after 48 days, Figure SX). Therefore, we can observe that the spectra only show signals related to the hydrogens and carbons present in the structure of the ionic liquid, with no signals related to the solubilization of CD-MOF in the ionic liquid.[3]

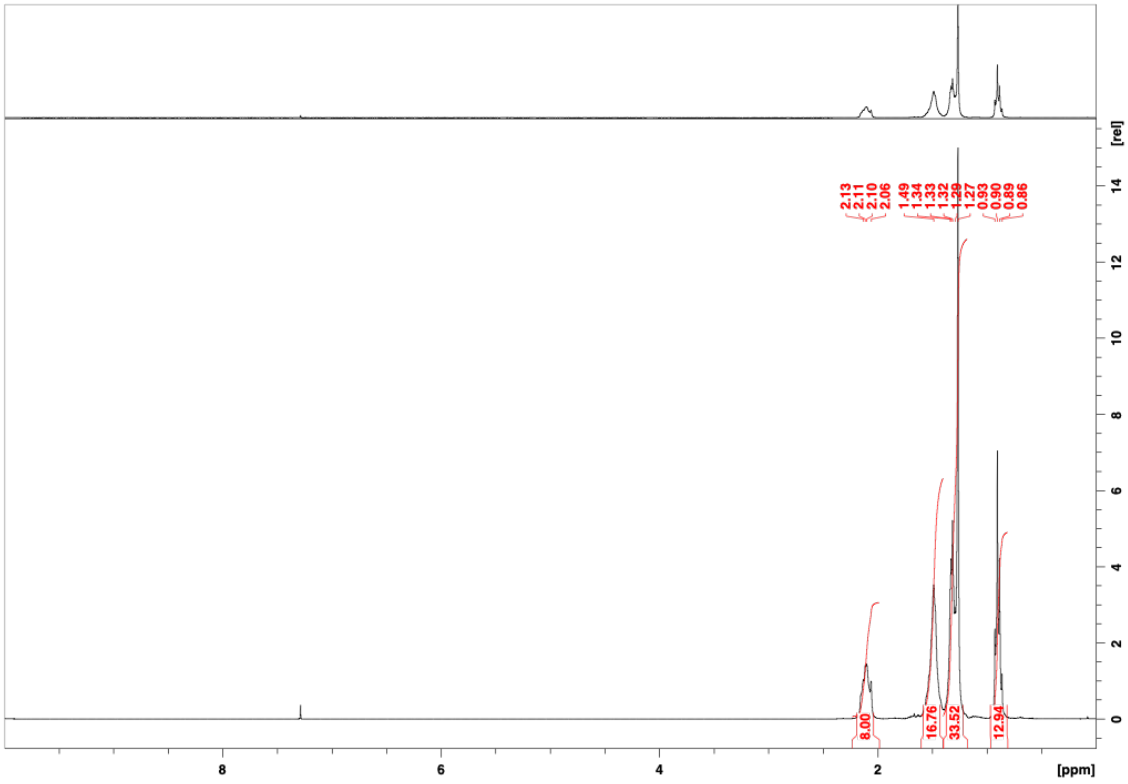

Figure S15: ^{1}H NMR of the upper phase of PoIL $[P_{6,6,6,14}][NTf_2]$ and CD-MOF-2 after complete phase separation in $CDCl_3$.

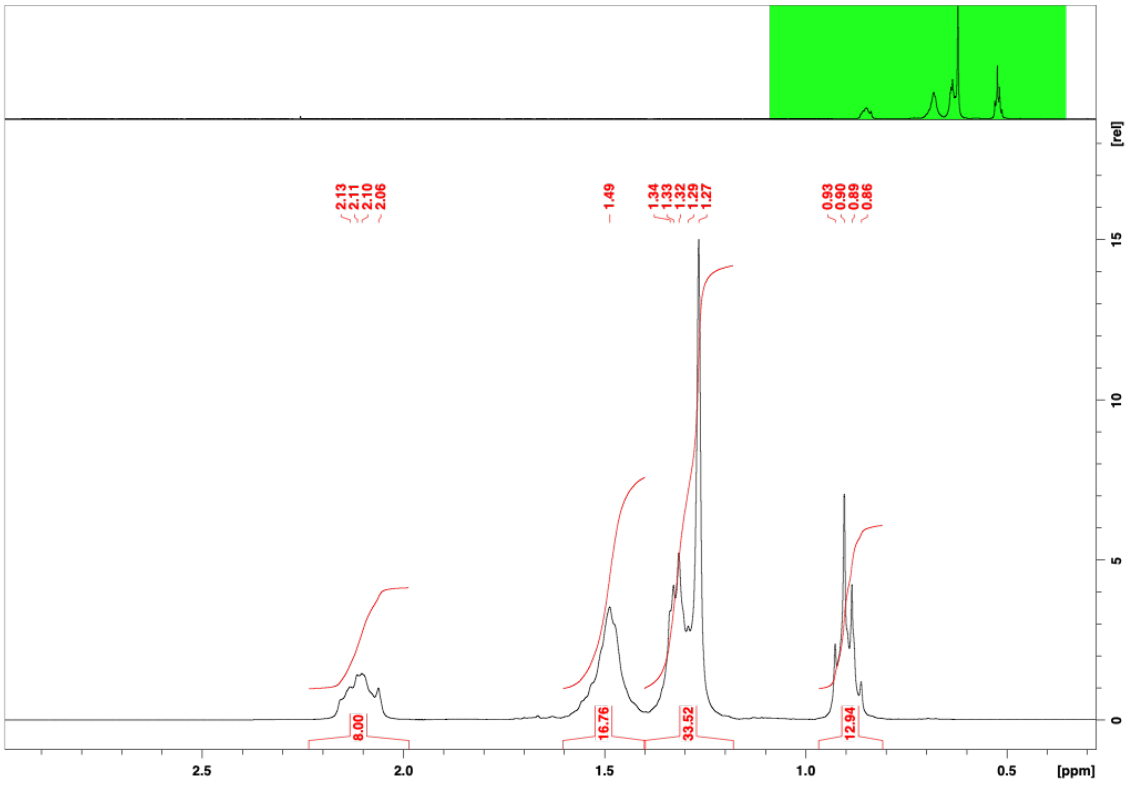

Figure S16: ^{1}H NMR of the upper phase of PoIL $[P_{6,6,6,14}][NTf_2]$ and CD-MOF-2 after complete phase separation (Zoom: 0-3 ppm) in $CDCl_3$.

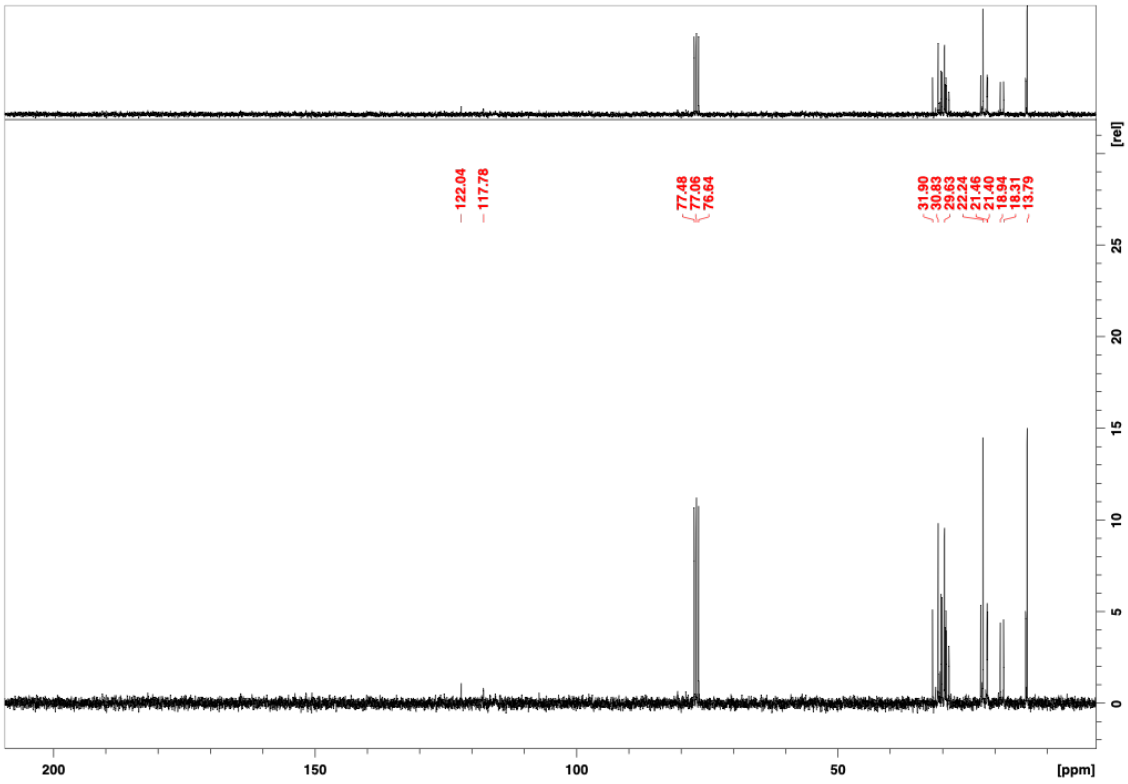

Figure S17: ^{13}C NMR of the upper phase of PoIL $[P_{6,6,6,14}][NTf_2]$ and CD-MOF-2 after complete phase separation in $CDCl_3$.

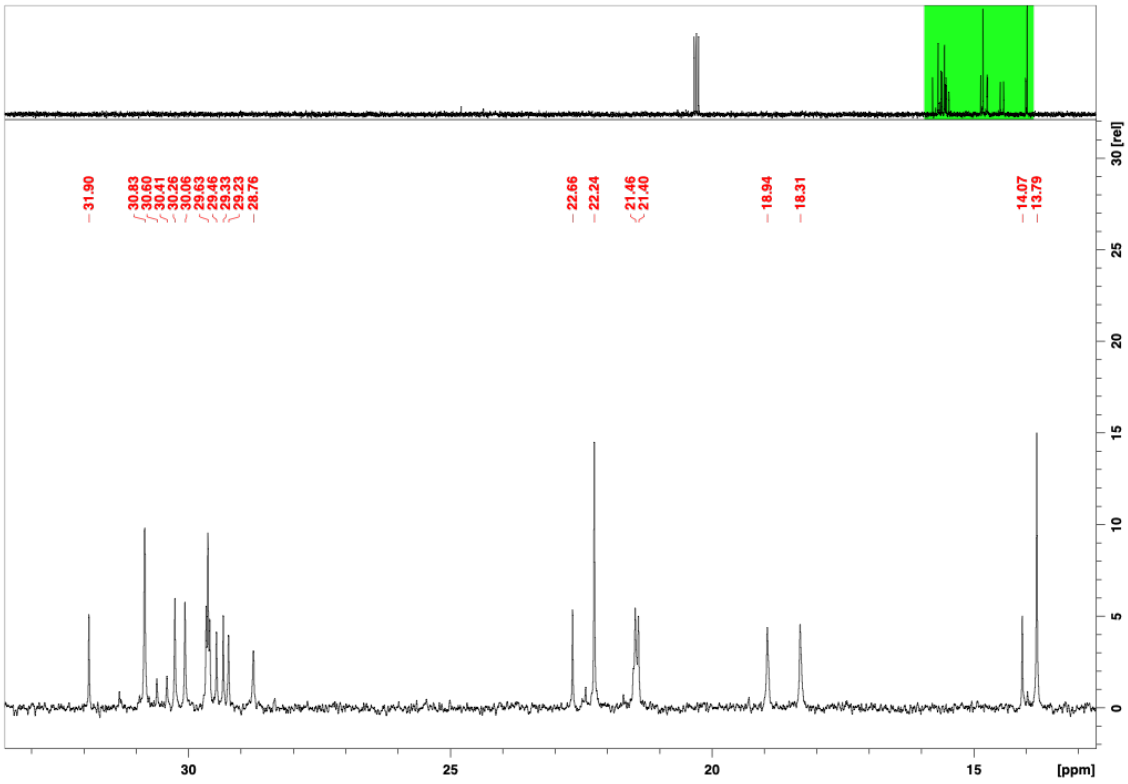

Figure S18: ^{13}C NMR of the upper phase of PoIL $[P_{6,6,6,14}][NTf_2]$ and CD-MOF-2 after complete phase separation (Zoom: 13-33 ppm) in $CDCl_3$.

References

(1) Avila, J.; Červinka, C.; Dugas, P.-Y.; Pádua, A. A.; Costa Gomes, M. Porous ionic liquids: Structure, stability, and gas absorption mechanisms. *Advanced Materials Interfaces* **2021**, *8*, 2001982.

(2) Avila, J.; Clark, R.; Pádua, A. A.; Gomes, M. C. Porous ionic liquids: beyond the bounds of free volume in a fluid phase. *Mater. Adv.* **2022**, *3*, 8848–8863.

(3) Arkhipova, E. A.; Ivanov, A. S.; Reshetko, S. S.; Aleshin, D. Y.; Maslakov, K. I.; Kupreenko, S. Y.; Savilov, S. V. Transport properties of nitrile and carbonate solutions of [P66614][NTf 2] ionic liquid, its thermal degradation and non-isothermal kinetics of decomposition. *Physical Chemistry Chemical Physics* **2021**, *23*, 23909–23921.